Oceanic Engineering International, Vol. 8, No. 2, 2004, pp. 91-103

System Identification of a SDOF System under Random Morison Loading using Lower and Higher Input R-MISO Models with Noise

S.K. Bhattacharyya[1,2,3] and R. Panneer Selvam[1]

[1] *Department of Ocean Engineering, Indian Institute of Technology Madras, India*
[2] *Faculty of Engineering and Applied Science, Memorial University of Newfoundland, St. John's, NL, Canada*
[3] *Institute for Ocean Technology, National Research Council Canada, St. John's, NL, Canada*

ABSTRACT

Reverse Multiple Input-Single Output (R-MISO) is a frequency domain system identification technique which can be utilized to identify the parameters of nonlinear equations of motion of a system from the measured random excitation and response data in the time domain. In this work, parameter estimation of a 'single degree of freedom' system with cubic nonlinear stiffness under random ocean wave excitation in the Morison regime, representing the dynamics of a submerged, moored spherical buoy, is investigated employing the R-MISO method. The focus is to propose and study the performance of higher input models for systems where their lower input counterparts are not sufficiently satisfactory in estimating some of the parameters and also to assess their relative performance in the presence of noise. Hydrodynamic drag and inertia coefficients and other system parameters are sought by the R-MISO method in two combinations of practical interest for which both lower and higher input models are feasible. Excitation and response data, including noise of chosen intensities, have been simulated in the numerical example and the R-MISO method applied to this data. Results indicate that the higher input models offer significant improvement in accuracy, though they may be somewhat less robust in the presence of noise.

Keywords: Drag coefficient, inertia coefficient, Morison equation, noise, nonlinear, random waves, reverse MISO, system identification, wave spectrum

1. INTRODUCTION

The response of a system to excitation depends on the parameters embedded in its equation of motion. Methods to estimate these parameters form the major concern of system identification (SI). In this paper, a relatively new nonlinear SI method, specifically the 'Reverse Multiple Input-Single Output' (R-MISO) method, has been employed with a nonlinear single-degree-of-freedom (SDOF) system representing the dynamics of a submerged, moored, spherical buoy under random wave loading in the Morison regime. The compliance of the system requires the relative velocity model of the Morison equation. The Pierson-Moskowitz (PM) spectrum is adopted in the numerical work to characterize the random ocean waves. In the numerical examples, the excitation and the response data with various 'noise' levels, given by signal-to-noise ratios (SNR) assuming Gaussian white noise (GWN), have been simulated and the R-MISO method applied to these 'noisy' data.

The R-MISO [Rice & Fitzpatrick 1991; Bendat & Piersol 1992; 1993] is a frequency domain method in which the roles of the input and output are reversed to form a MISO model. Conditioned spectral density functions of the input and output are used in its algorithm [Bendat 1976]. The advantages of this method are that it is non-iterative, robust, and computationally light and requires no starting estimates. It has found application in a variety of nonlinear systems, namely, Duffing, van der Pol, Mathieu and dead-band systems [Bendat *et al* 1992]. Early effort of the application of the R-MISO method in the area of offshore engineering is due to Yim & Bartel [1994] and Spanos & Lu [1995]. Recently, Narayanan *et al* [1998; 2000], Panneer Selvam *et al* [1999] and Panneer Selvam & Bhattacharyya [2001] made attempts to use the R-MISO method in ocean engineering systems such as a moored buoy under random ocean waves. In these works, the focus has been to determine the drag and inertia coefficients embedded in the Morison equation, in addition to the system parameters, including nonlinear mooring line stiffness using different R-MISO models.

In this paper we propose higher input R-MISO models for SDOF systems where their lower input counterparts are not sufficiently accurate in estimating some of the parameters and we study the relative performance of lower versus higher input models. A major concern of SI is to assess the performance of algorithms in the presence of noise in both the input and output. The effect of noise has been studied in this paper with the aim to assess how the higher input models behave in the presence of noise in comparison to their lower input counterparts.

2. SYSTEM MODEL

We consider the problem of SI associated with a nonlinear SDOF system under random wave excitation whose equation of motion is given by

$$m\ddot{x}+c\dot{x}+kx+Kx^3=f(t) \tag{1}$$

where m, c, k and K represent the mass, linear damping (dash-pot) constant, linear stiffness (spring) constant, and cubic nonlinear stiffness (spring) constant, respectively. The wave excitation, $f(t)$, is given by the well-known relative velocity model of the Morison equation [Chakrabarti 1987]

$$f(t)=\rho V\dot{u}+C_a\rho V(\dot{u}-\ddot{x})+0.5C_D\rho\ A|u-\dot{x}|(u-\dot{x}) \tag{2}$$

where V is the volume, A is the projected cross-sectional area normal to the direction of flow, C_a is the added mass coefficient ($= C_M - 1$), C_M is the inertia coefficient, C_D is the drag coefficient, ρ is the density of water and u and $\dot{u}$ are the water particle velocity and acceleration, respectively. The system considered is shown in figure 1. The R-MISO method can be used to estimate the linear system parameters, namely m, c and k, the nonlinear stiffness parameter K as well as the hydrodynamic coefficients C_D and C_M under spectral wave loading by formulating different 'Multiple Input-Single Output' models. The algorithm of the R-MISO method is presented in the Appendix.

3. FORMULATION OF SI

In formulating the SI for the system given by equations (1) and (2), we consider two different cases as given below.

(a) Case 1

In this case one needs to know the inertia coefficient (C_M) of the system *apriori*. We rearrange equation (1), noting equation (2), as

$$\begin{aligned}&(m+C_a\rho V)\ddot{x}+c\dot{x}+kx+Kx^3-0.5C_D\rho A|u-\dot{x}|(u-\dot{x})\\&=C_M\rho V\dot{u}\\&=\bar{f}(t)\end{aligned} \tag{3}$$

and take the Fourier Transform (FT) of this equation as

$$A_L(\omega)X_L(\omega)+A_{NL1}(\omega)X_{NL1}(\omega)+A_{NL2}(\omega)X_{NL2}(\omega)=\bar{F}(\omega) \tag{4}$$

where

$$A_L=k+i\omega c-\omega^2 m' \tag{5}$$

$$A_{NL1}=K \tag{6}$$

$$A_{NL2}=0.5C_D\rho A \tag{7}$$

$$m'=m+C_a\rho V \tag{8}$$

and X_L, X_{NL1}, X_{NL2} and $\bar{F}$ are FTs of the inputs x, x^3, $-|u-\dot{x}|(u-\dot{x})$ and $\bar{f}$ respectively and m' is the virtual mass of the system. Equation (4) is a "Three Input-Single Output" model (see figure 1(a)) with one linear and two nonlinear inputs. In equation (5), A_L is the linear transfer function (or frequency response function) as it is associated with linear input (x). Similarly, A_{NL1} and A_{NL2} are the transfer functions associated with nonlinear inputs x^3 and $-|u-\dot{x}|(u-\dot{x})$, respectively. In the above, the subscript 'L' stands for a quantity pertaining to a 'Linear' input and the subscript 'NL' stands for a quantity pertaining to a 'Nonlinear' input.

The linear parameters (i.e. k, c and m') can be obtained from equation (5) as

$$k=A_L(0) \tag{9}$$

$$c=\frac{\mathrm{Im}\{A_L(\omega)\}}{\omega} \tag{10}$$

$$m'=\frac{k-\mathrm{Re}\{A_L(\omega)\}}{\omega^2} \tag{11}$$

Alternatively, from the plot of $|A_L|$ versus ω, one can obtain the parameters as

$$k=|A_L(0)| \tag{12}$$

$$c=\frac{|A_L(\omega_n)|}{\omega_n} \tag{13}$$

$$\omega_n=\sqrt{k/m'} \tag{14}$$

Since the peak (minima) of the $|A_L|$ curve corresponds to $\omega=\omega_n$ (natural frequency) for small damping ratios, one can easily obtain the virtual mass m'. From the plots of A_{NL1} and A_{NL2}, which are constants for all ω, the parameters K and C_D can be readily obtained from equations (6) and (7).

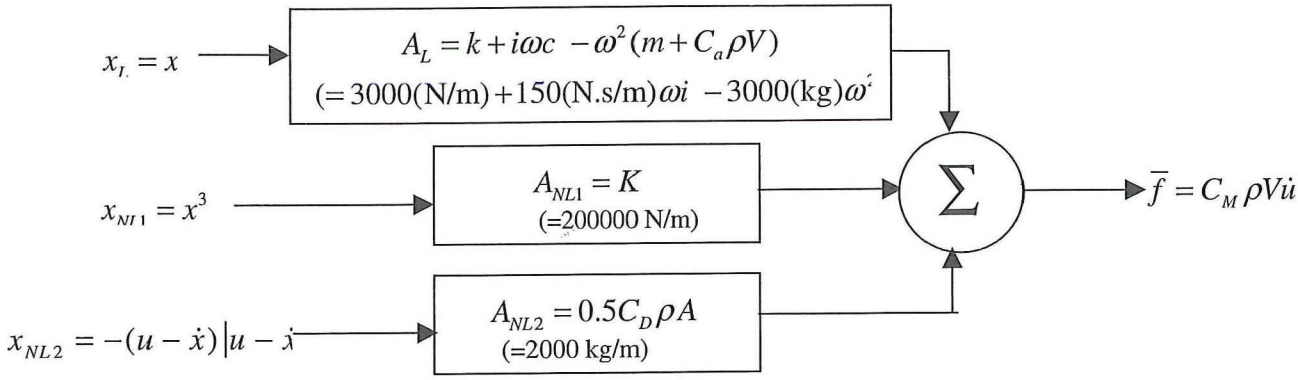

Figure 1(a). Three input-single output model: Case 1(a).

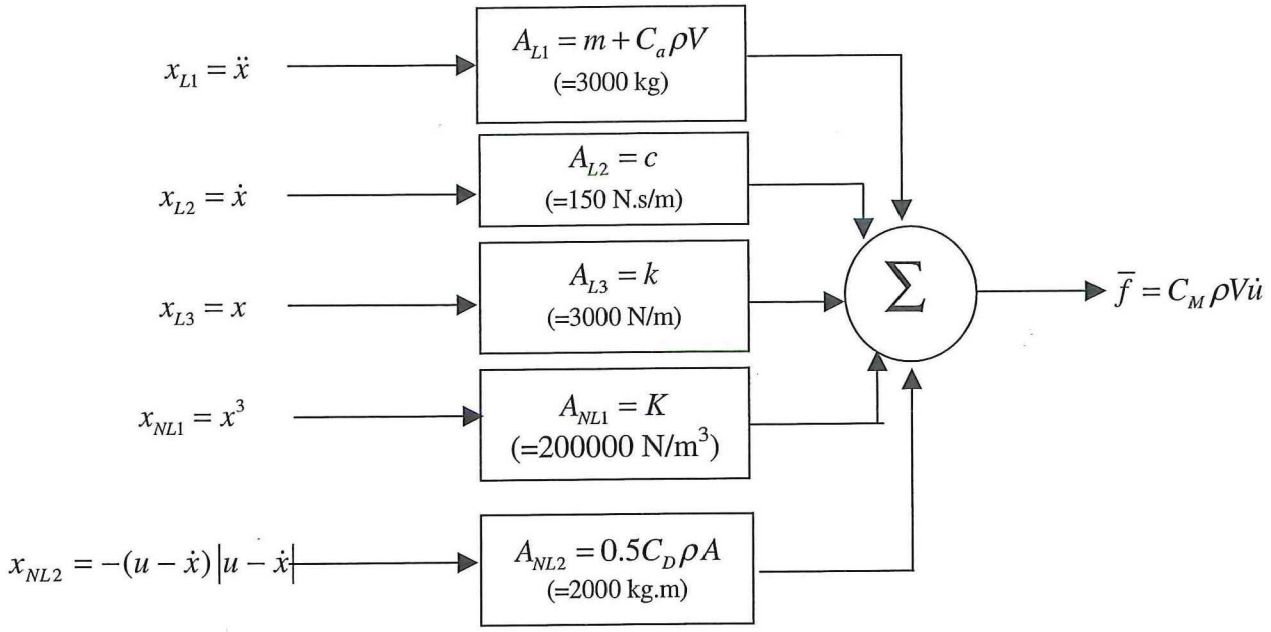

Figure 1(b). Five input-single output model: Case 1(b).

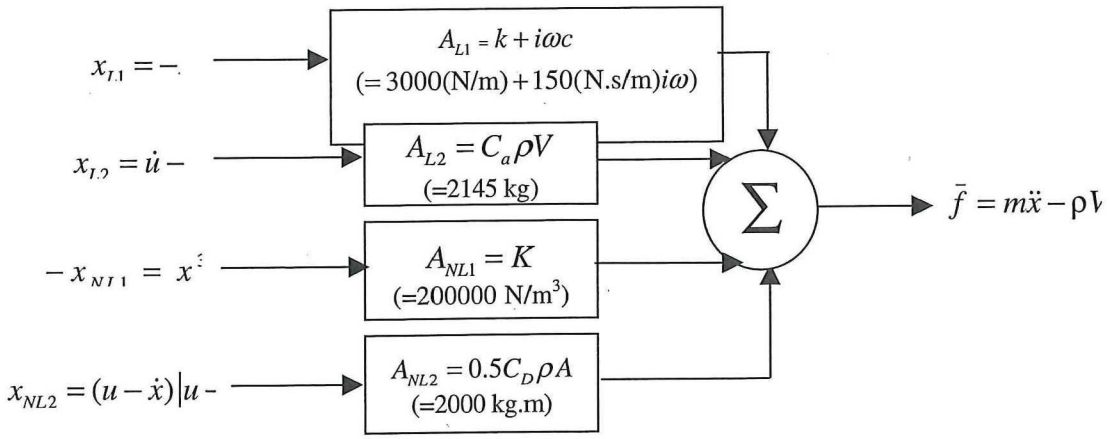

Figure 2(a). Four input-single output model: Case 2(a).

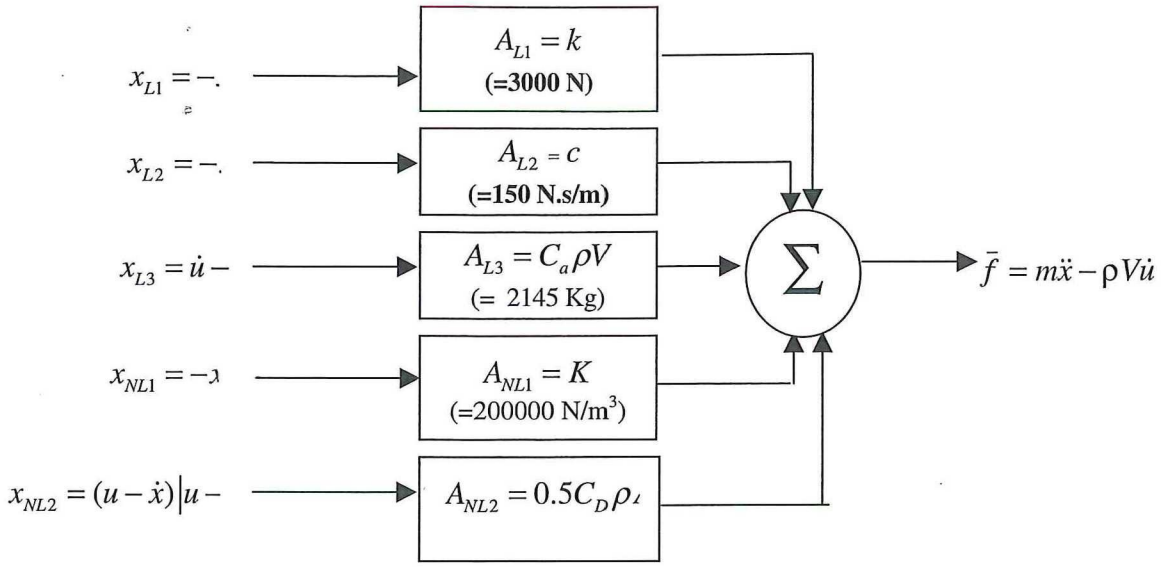

Figure 2(b). Five input-single output model: Case 2(b).

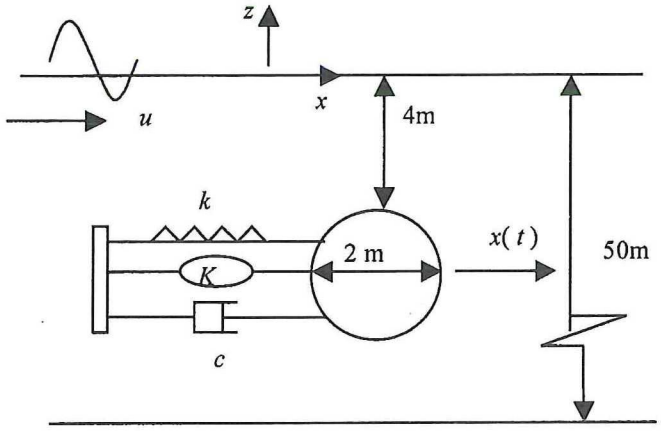

Figure 3. A compliant SDOF system subjected to wave excitation.

One can take the FT of equation (3) in an alternative way as follows.

$$\begin{aligned} &A_{L1}(\omega)X_{L1}(\omega) + A_{L2}(\omega)X_{L2}(\omega) \\ &+ A_{L3}(\omega)X_{L3}(\omega) + A_{NL1}(\omega)X_{NL1}(\omega) \\ &+ A_{NL2}(\omega)X_{NL2}(\omega) \\ &= \bar{F}(\omega) \end{aligned} \tag{15}$$

where

$$A_{L1} = m' \tag{16}$$

$$A_{L2} = c \tag{17}$$

$$A_{L3} = k \tag{18}$$

$$A_{NL1} = K \tag{19}$$

$$A_{NL2} = 0.5 C_D \rho A \tag{20}$$

and $X_{L1}, X_{L2}, X_{L3}, X_{NL1}, X_{NL2}$ and $\bar{F}$ are FTs of the inputs $\ddot{x}$, $\dot{x}$, x, x^3, $-|u - \dot{x}|(u - \dot{x})$ and $\bar{f}$, respectively. Equation (15) is a 'Five input - Single Output' model (see figure 1(b)) with three linear and two nonlinear inputs. From the A_{L1}, A_{L2}, A_{L3}, A_{NL1} and A_{NL2} plots, which are constants for all ω, the parameters m', c, k, K and C_D can readily be obtained from equations (16) through (20).

(b) Case 2

In this case one needs to know the mass (m) of the system *apriori*. We rearrange equation (1), noting equation (2), as

$$\begin{aligned} &-(c\dot{x}+kx)+C_a\rho V(\dot{u}-\ddot{x}) \\ &-Kx^3+0.5C_D\rho A|u-\dot{x}|(u-\dot{x}) \\ &=m\ddot{x}-\rho V\dot{u} \\ &=\bar{f}(t) \end{aligned} \tag{21}$$

and take the Fourier Transform (FT) of this equation as

$$\begin{aligned} &A_{L1}(\omega)X_{L1}(\omega)+A_{L2}(\omega)X_{L2}(\omega) \\ &+A_{NL1}(\omega)X_{NL1}(\omega)+A_{NL2}(\omega)X_{NL2}(\omega) \\ &=\bar{F}(\omega) \end{aligned} \tag{22}$$

where

$$A_{L1}=k+i\omega c \tag{23}$$

$$A_{L2}=C_a\rho V \tag{24}$$

$$A_{NL1}=K \tag{25}$$

$$A_{NL2}=0.5C_d\rho A \tag{26}$$

and $X_{L1}, X_{L2}, X_{NL1}, X_{NL2}$ and $\bar{F}$ are FTs of the inputs $-x, \dot{u}-\ddot{x}, -x^3, |u-\dot{x}|(u-\dot{x})$ and $\bar{f}$ respectively. Equation (22) is a 'Four Input - Single Output' model (see figure 2(a)) with two linear and two nonlinear inputs. From equation (23), it is seen that the real part of A_{L1} is a constant and equals k while its imaginary part is a linear function of ω with proportionality constant as c. Hence k and c can easily be obtained from A_{L1}. From the plots of A_{L2}, A_{NL1}, and A_{NL2}, which are constants for all ω, the parameters C_M (= 1 + C_a), K and C_D can readily be obtained from equations (24) through (26).

One can take the FT of equation (21) in an alternative way as

$$\begin{aligned} &A_{L1}(\omega)X_{L1}(\omega)+A_{L2}(\omega)X_{L2}(\omega) \\ &+A_{L3}(\omega)X_{L3}(\omega)+A_{NL1}(\omega)X_{NL1}(\omega) \\ &+A_{NL2}(\omega)X_{NL2}(\omega) \\ &=\bar{F}(\omega) \end{aligned} \tag{27}$$

where

$$A_{L1}=k \tag{28}$$

$$A_{L2}=c \tag{29}$$

$$A_{L3}=C_a\rho V \tag{30}$$

$$A_{NL1}=K \tag{31}$$

$$A_{NL2}=0.5C_d\rho A \tag{32}$$

and $X_{L1}, X_{L2}, X_{L3}, X_{NL1}, X_{NL2}$ and $\bar{F}$ are FTs of the inputs $-x, -\dot{x}, \dot{u}-\ddot{x}, -x^3, |u-\dot{x}|(u-\dot{x})$ and $\bar{f}$ respectively. Equation (27) is a 'Five Input - Single Output' model (see figure 2(b)) with three linear and two nonlinear inputs. From the plots of A_{L1}, A_{L2}, A_{L3}, A_{NL1} and A_{NL2}, which are constants for all ω, the parameters k, c, C_M, K and C_D can readily be obtained from equations (28) through (32).

The R-MISO algorithm of the Appendix can be used to compute the transfer functions A_L and A_{NL} in equations (4), (15), (22) and (27) for the Cases 1(a), 1(b), 2(a) and 2(b), respectively.

4. NUMERICAL EXAMPLE

We consider an example problem of a submerged spherical buoy of 2 m diameter (see figure 3) with the following assumed parameters: m = 855 kg, c = 150 N.s/m, k = 3000 N/m, K = 2×10^5 N/m^3, C_a = 0.5, C_D = 1.2434, A = π m^2, V = 4.1888 m^3 and ρ = 1025 kg/m^3. The buoy is located 5 m below the water surface at a depth of 50 m. The narrow band PM spectrum $S_{\eta\eta}$ of wave elevation (η) characterizes the random wave surface and is given by

$$S_{\eta\eta}(\omega)=5\sigma^2\omega^{-5}\omega_0^4\exp[-1.25(\omega/\omega_0)^{-4}], \quad \sigma=H_s/4 \tag{33}$$

where a significant wave height (H_s) of 5 m and peak frequency (ω_0) of 0.4 rad/s are adopted in the calculations. Time domain simulation of η from the spectrum has been carried out by a spectrally deterministic random phase method [Chakrabarti 1987]. The time series of u for this problem have been simulated from $S_{\eta\eta}$ in conjunction with the linear wave theory. The time step (Δt = 0.1s) has been chosen in order to obtain reasonably good resolution of the response (x) so that $\dot{x}$ and $\ddot{x}$ could be computed accurately by successive differentiation using a finite difference formula. Similarly $\dot{u}$ has been found by differentiating the time series of u. All auto- and cross-spectra (see Appendix) were calculated based on 8 records of 512 samples (i.e. 4096 data points), with a sampling rate of 10Hz (Δt = 0.1s). A total of 10, 15 and 25 spectra are needed in the R-MISO algorithm for three (Case 1(a)), four (Cases 1(b) and 2(a)) and five (Case 2(b)) input models respectively.

The 'real' data, which are obtained from physical experiments, invariably contain noise. The effect of noise on the prediction of parameters is of interest in the practical application of any SI method. The effect of 'noise' in the time series of the inputs as well as the output on the proposed SI models needs to be examined. Noise usually is assumed to be uncorrelated to both the inputs and output. It is introduced during measurement, simulation, or during data or signal processing. In this study, noise is introduced in each of the inputs as well as in the output and SI is performed on the

'noisy' data. A Gaussian white noise is added to a particular signal such that the signal to noise ratio (SNR) of a specific decibel (dB) is achieved. SNR in dB is given by

$$SNR = 10 \log_{10} \frac{\sigma_s}{\sigma_n} \tag{34}$$

where σ_s and σ_n are the root mean square (equals standard deviation for a zero mean process) values of the signal and noise, respectively. Three different SNR values (30 dB, 20 dB and 10 dB) are chosen for numerical study. The data without noise corresponds to SNR = ∞. These values of SNR are consistent with the range of values considered by Spanos & Lu [1995] and Hac & Spanos [1990] in the context of SI with noise.

Typically, in an experiment, either one measures x and calculates $\dot{x}$ and $\ddot{x}$ by successive differentiation of the time series of x, or one measures $\ddot{x}$ and calculates $\dot{x}$ and x by successive integration of the time series of $\ddot{x}$. The same holds for u and $\dot{u}$. In practice, the quantity that will be measured depends upon the convenience and the availability of the instrumentation. However, since noise is generally present in an experiment, one has to be aware that differentiation of a signal amplifies high frequency noise components whereas integration of a signal removes them. The data filtering will therefore have a significant role depending upon the choice of the measured quantity.

5. RESULTS AND DISCUSSION

The spectra of η and u are shown in figure 4. The spectrum of x is shown in figure 5. The time series of the excitation (f in equation 2) and response (x) of the system have been simulated for $K = 2\times10^5$ N/m^3 and $K = 0$ and are shown in figure 6, which clearly bring out the strong effect of the cubic nonlinear spring stiffness (K) on the system response (x). For more details of this problem, Panneer Selvam & Bhattacharyya [2001] may be consulted. The time series and spectra of velocity and acceleration responses for $K = 2\times10^5$ N/m^3 are shown in figure 7.

The SI results without noise for lower as well as higher input models are summarized in table 1 for both Case 1 and Case 2. The coherence functions in Cases 1(a) (3-input) and 1(b) (5-input) with noise are shown in figure 8 which show that in the frequency range of interest, the cumulative values are almost unity, showing that all parameters of significance are accounted for in the SI model. For transfer functions that are independent of frequency, all SI results reflect a mean of all values in the frequency range of 0.2 to 1.4 rad/s, which satisfactorily covers the effective range of the spectra of η and u in figure 4. These results bring out several conclusions and features of the problem. Firstly, the lower input models (Cases 1(a) and 2(a)) poorly estimate the linear damping constant, c, but its estimate dramatically improves once the velocity response ($\dot{x}$) is treated as one of the additional inputs in the corresponding higher input models (Cases 1(b) and 2(b), respectively). The errors in damping are 4.53% and under 1% for the higher input models as compared to 55% and 98% in the corresponding lower input models, respectively. Clearly, this is a significant advantage of the higher input models over their lower input counterparts. Secondly, the lower input model of Case 1 underestimates the virtual mass by 22% and this error also dramatically decreases to less than 1% using the corresponding higher input model. This again is because the acceleration response ($\ddot{x}$) is treated as one of the independent inputs in the higher input models. Thirdly, the higher input model of Case 1 marginally improves the estimates of both linear and nonlinear stiffness constants as compared to the corresponding lower input model. For Case 2, these stiffness constants are already quite accurate (under 1% error) for the lower input model and no benefit accrues by using the higher input model. Fourthly, the drag coefficient is uniformly estimated very accurately in both cases by both the lower and higher input models. Thus, in general, it can be stated that the higher input R-MISO models can significantly improve the overall performance of parameter estimation.

The SI results with noise for lower as well as higher input models are summarized in table 2 for both Case 1 and Case 2. In presenting these results, the percentage error of mean over the appropriate frequency range with respect to the reference value is indicated for a particular parameter. However, error of mean is not sufficiently representative of the accuracy and for a particular choice of spectral analysis parameters it can be fortuitously but misleadingly 'accurate'. Therefore a 'coefficient of variation' or 'cov', defined as '% cov' = 100 × (standard deviation/mean), is also given in table 2 in addition to the error of mean.

The results in table 2 bring out several conclusions and features of the problem. Firstly, SNR = 30 dB affects the SI estimates only marginally in all cases. It is therefore a low noise level. Secondly, SNR = 20 dB affects the SI estimates of lower input models (Cases 1(a) and 2(a)) 'somewhat'. The worst deterioration of estimate is for linear stiffness constant (k) in Case 2(a) which has mean error of 5.8% and cov of 10.23% compared to corresponding values of under 1% for both at SNR = 30 dB. Clearly, the estimates of lower input models at SNR = 20 dB are still accurate enough for practical applications. Thirdly, SNR = 20 dB affects the SI estimates of higher input models (Cases 1(b) and 2(b)) 'significantly'. The linear stiffness constant (k) in Case 1(b) has mean error of 30.8% (as against 6.9% for Case 1(a)) and in Case 2(b) it has mean error of 13.7% (as against 5.8% for Case 2(a)). The nonlinear linear stiffness constant (K) in Case 2(b) has a mean error of 32.07% (as opposed to 4.38% for Case 2(a)). The drag coefficient (C_D) in Case 2(b) has mean error of 32.7% (as compared to 4.82% for Case 2(a)). Clearly, the estimates of higher input models at SNR = 20 dB are unacceptably erroneous for practical applications. The results for SNR = 10 dB reinforce the same conclusions.

Thus, in general, it can be stated that the higher input R-MISO models, while being significantly superior to the lower input models with low to moderate noise levels, are less robust than the lower input models in the presence of high noise levels.

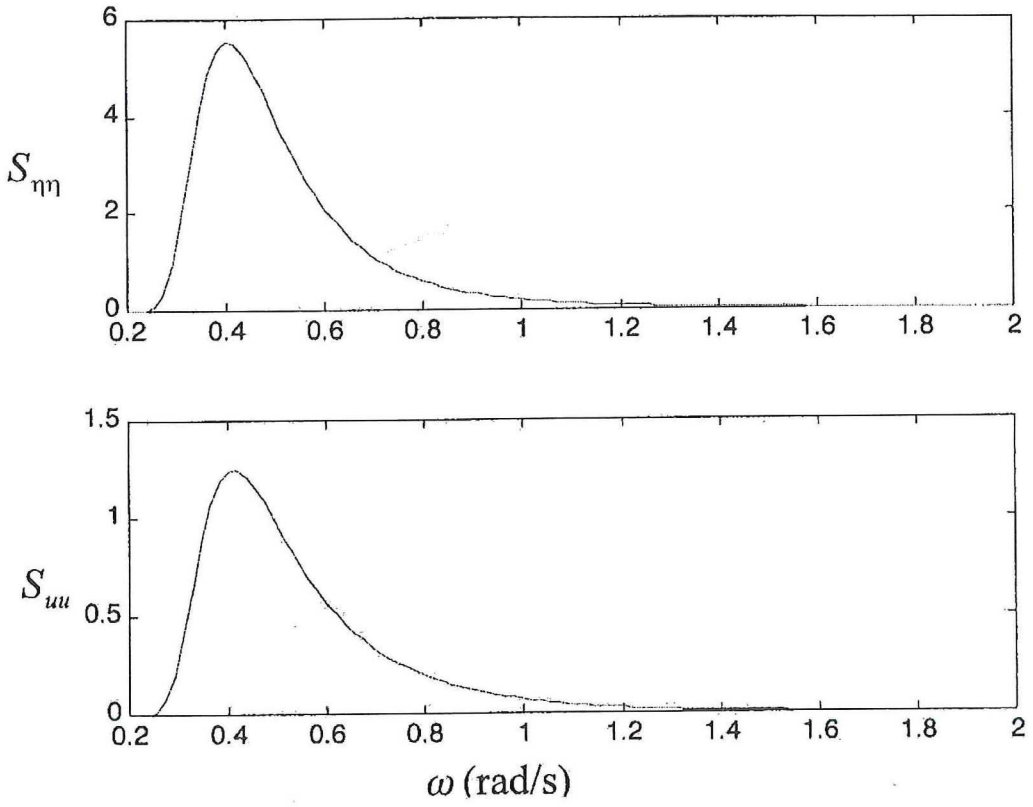

Figure 4. PM spectrum ($S_{\eta\eta}$ in m^2s) used in simulation and the spectrum of water particle velocity(S_{uu} in m^2/s) at centre of the sphere ($z = -5$m, see figure (3)).

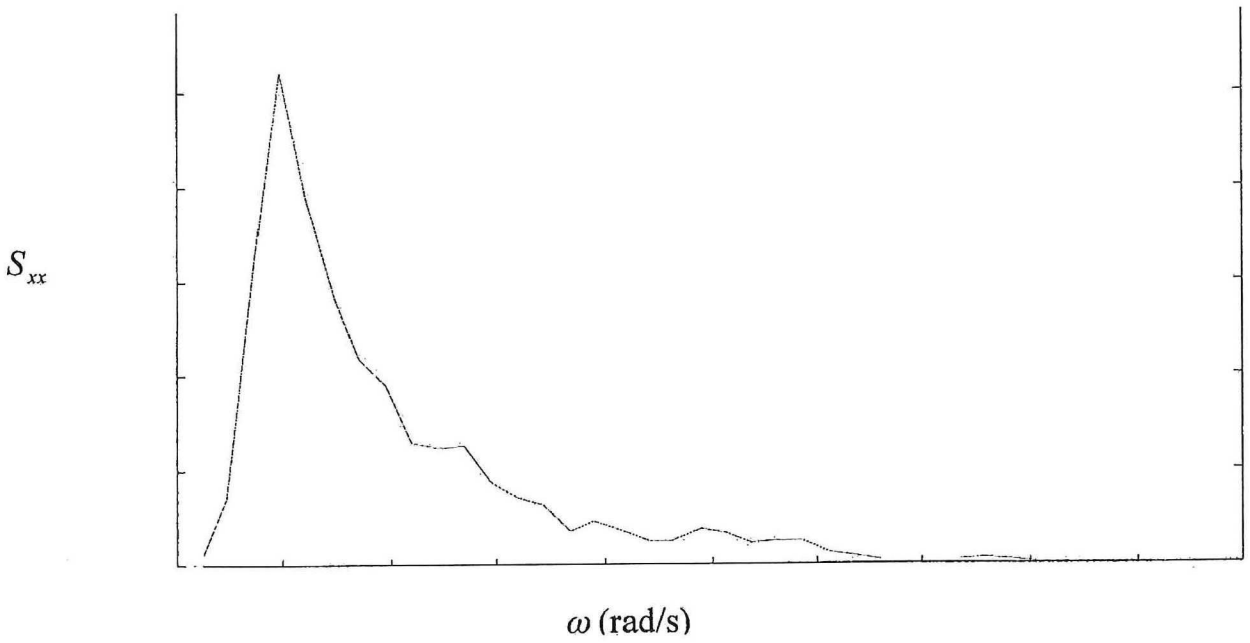

Figure 5. Spectrum of the response (S_{xx} in m^2s) of the spherical buoy.

Reference Values	Estimated values (% Error)		Reference Values	Estimated values (% Error)	
	Case 1a (3-input)	Case 1b (5-input)		Case 2a (4-input)	Case 2b (5-input)
m' (3000 kg)	2344 (–21.87%)	2999 (<1%)	C_M (1.5)	1.4955 (<1%)	1.4974 (<1%)
c (150 N.s/m)	66.64 (–55.6%)	143 (–4.53%)	c (150 N.s/m)	2.7 (–98%)	143 (<1%)
k (3000 N/m)	2836 (–5.47%)	2993 (<1%)	k (3000 N/m)	2991 (<1%)	3004 (<1%)
K (200000 N/m^3)	194900 (–2.55%)	199957 (<1%)	K (200000 N/m^3)	199444 (<1%)	199609 (<1%)
C_D (1.2434)	1.2254 (–1.44%)	1.2430 (<1%)	C_D (1.2434)	1.2398 (<1%)	1.241 (<1%)

Table 1. SI results: lower vs. higher input models without noise.

Parameter	Case	% Error of mean *w.r.t.* reference values (% cov)			
		SNR: ∞	30 dB	20 dB	10 dB
k	1(a) (3 input)	–5.47 (-)	–5.63 (-)	–6.9 (-)	–13 (-)
	1(b) (5 input)	<1 (1.1)	5.05 (11.06)	30.8 (21.2)	3.23 (41)
	2(a) (4 input)	<1 (<1)	<1 (<1)	–5.8 (10.23)	–77 (97)
	2(b) (5 input)	<1 (4)	7.9 (12.23)	13.7 (32.44)	–51.2 (>100)
K	1(a)	–2.55 (4.15)	–2.54 (4.17)	–2.5 (4.37)	–6.36 (7.57)
	1(b)	<1 (<1)	<1 (<1)	<1 (<1)	–5.1 (8.8)
	2(a)	<1 (<1)	<1 (<1)	–4.38 (9.25)	–41.5 (17.21)
	2(b)	<1 (<1)	–4.74 (5.89)	–32.07 (22)	–43.4 (23.31)
C_D	1(a)	–1.44 (7.51)	–1.39 (7.52)	<1 (7.65)	<1 (10.1)
	1(b)	<1 (<1)	<1 (<1)	<1 (1.1)	<1 (11.04)
	2(a)	<1 (<1)	<1 (<1)	–4.82 (9.14)	43 (20.7)
	2(b)	<1 (<1)	–4.81 (5.86)	–32.7 (22)	–47.24 (20.47)

Table 2. SI results: lower vs. higher input models with noise levels.

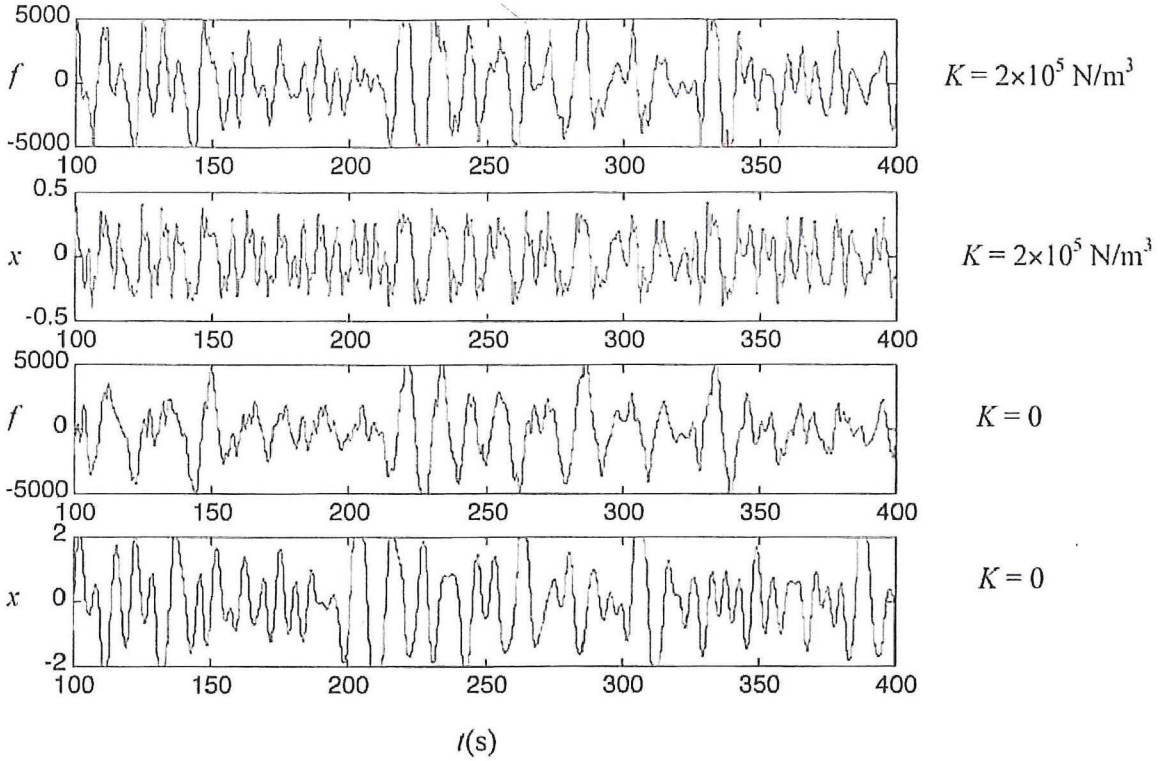

Figure 6. Wave excitation (f in N) force and response (x in m) of the spherical buoy.

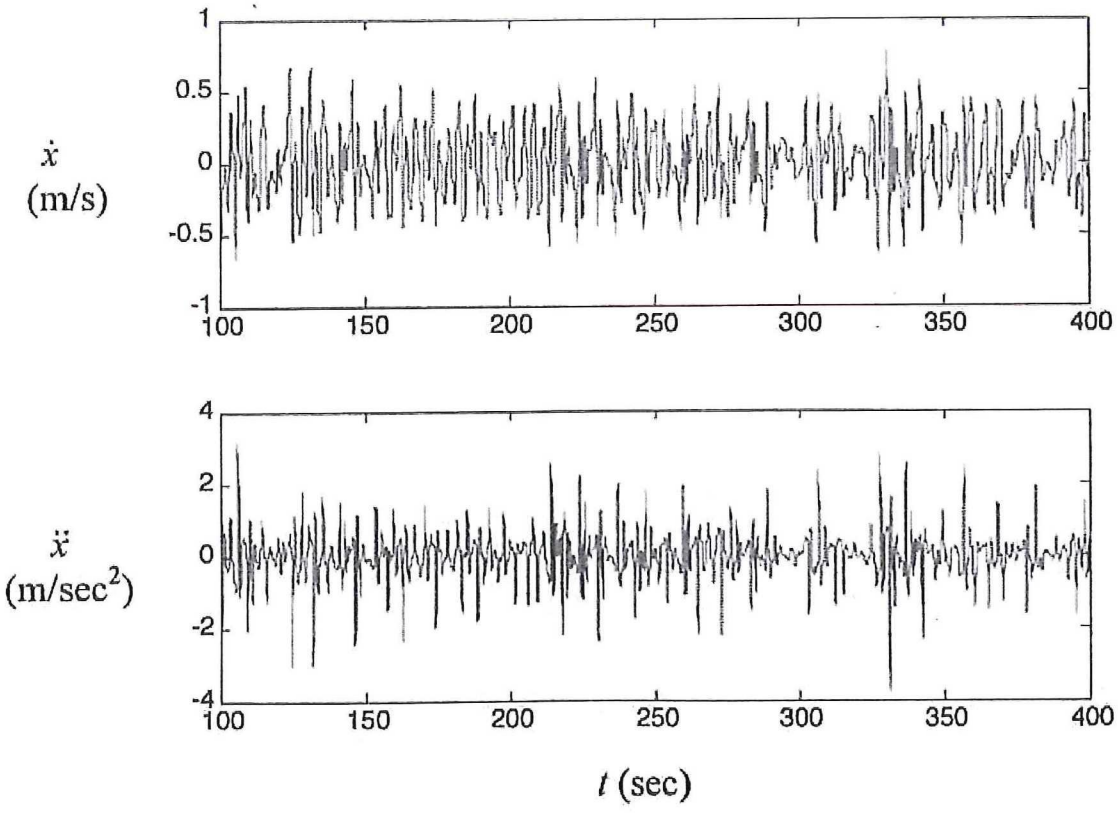

Figure 7(a). Time series.

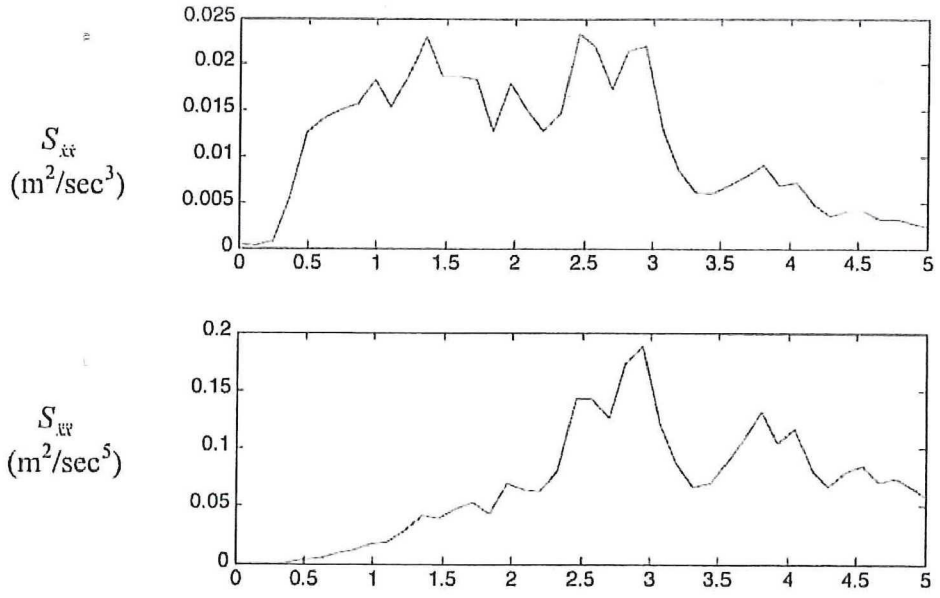

Figure 7(b). Spectra.

Figure 7. Time series and spectra of velocity and acceleration of the spherical buoy.

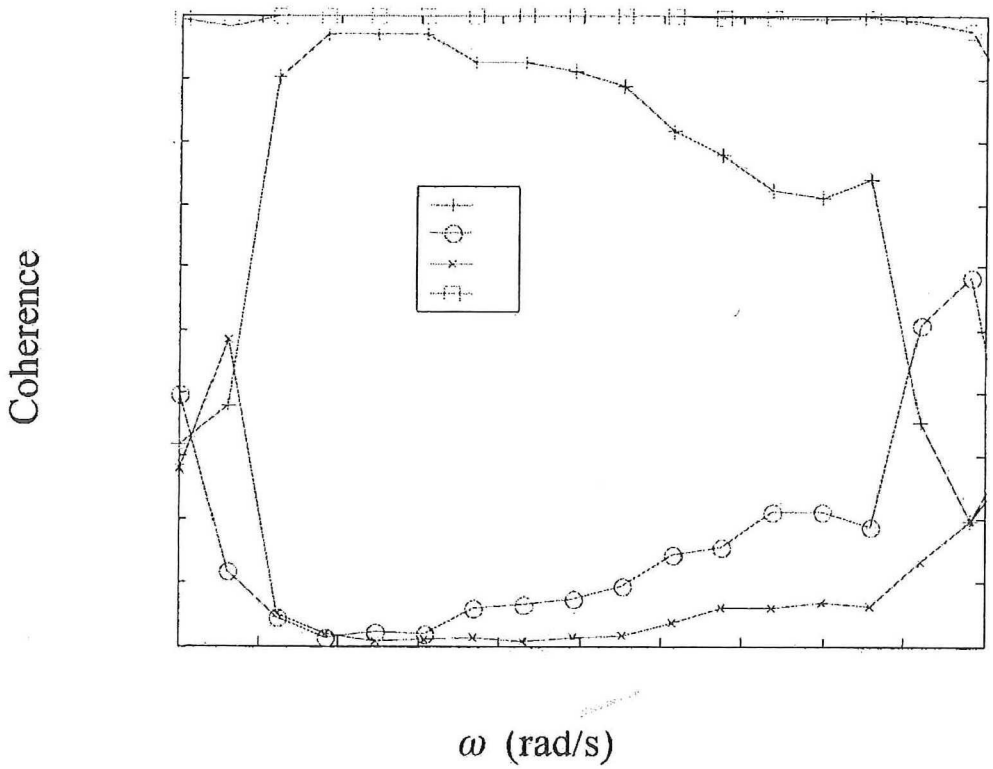

Figure 8(a). Case 1(a).

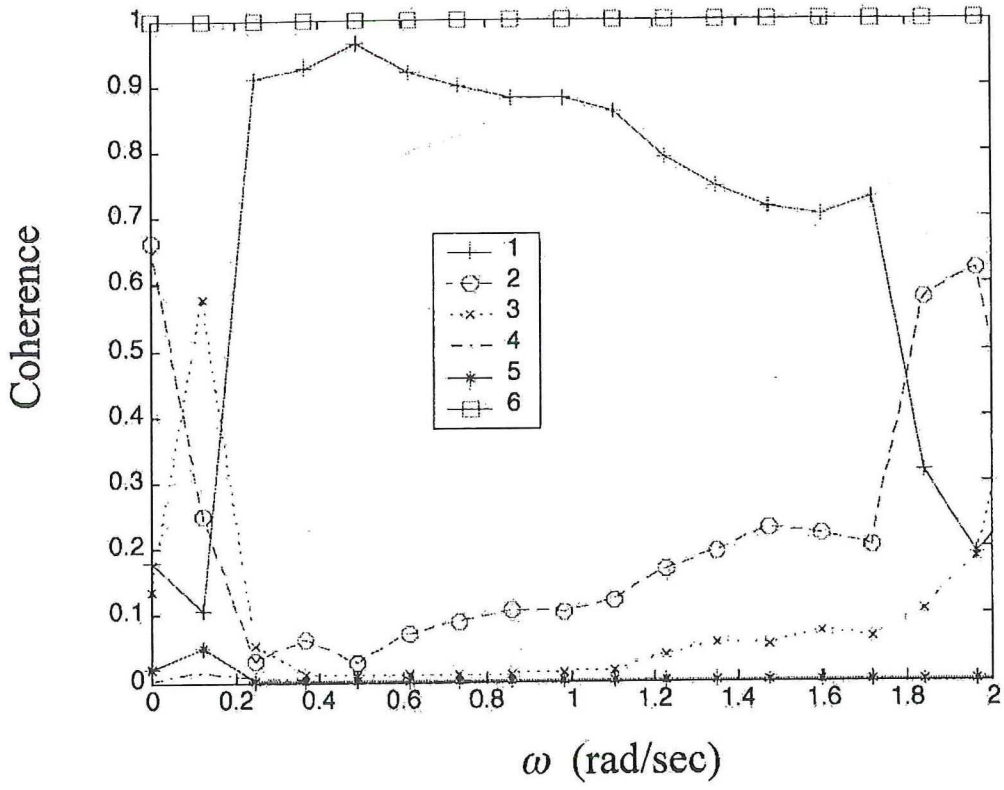

$1:\gamma^2_{x_1y}\quad 2:\gamma^2_{x_2y}\quad 3:\gamma^2_{x_3y}\quad 4:\gamma^2_{x_4y}\quad 5:\gamma^2_{x_5y}\quad 6:\sum_{i=1}^{5}\gamma_{x_iy}$

$(x_1 = x_{L1}, x_2 = x_{L2}, x_3 = x_{L3}, x_4 = x_{NL1}, x_5 = x_{NL2}; y = f)$

Figure 8(b). Case 1(b).

Figure 8. Coherence plots for Case 1 with SNR = 30 dB.

6. CONCLUSION

The performance of the R-MISO method has been investigated for parameter identification of a nonlinear, SDOF ocean engineering system in random ocean waves using lower and higher order models with 'noisy' input and output time series. The relative velocity model of the Morison equation gives the hydrodynamic loading on the system and the random waves are represented by wave spectra. The focus has been on the identification of all the unknown parameters embedded in the equation of motion of the system. Two problems have been formulated and the two SI models, one 'lower input' and the other 'higher input', have been proposed for each of the problems leading to Three, Four and Five Input - Single Output models. Limited numerical study undertaken suggests that while the higher input R-MISO models are significantly superior to the lower input models with low to moderate noise levels, they are less robust than the lower input models in the presence of high noise levels.

REFERENCES

Bendat, J.S. 1976 System identification from multiple input/output data. *Journal of sound and vibration*, **49** (3), 293-308.

Bendat, J.S., Palo, P.A. & Coppolino, R.N. 1992 A general identification technique for nonlinear differential equations of motion. *Probabilistic engineering mechanics*, **7**, 43-61.

Bendat, J.S. & Piersol, A.G. 1993 *Engineering applications of correlation and spectral analysis.* New York: Wiley Interscience.

Chakrabarti, S.K. 1987 *Hydrodynamics of offshore structures.* Computational Mechanics Publications.

Hac, A. & Spanos, P.D. 1990 Time domain method for parameter identification. *Journal of sound and vibration,* **112**, 281-285.

Narayanan, S., Yim, S.C.S., & Palo, P.A. 1998 Nonlinear system identification of a moored structural system. In *Proceedings of the 8th international offshore and polar engineering conference* (ISOPE' 98), Montreal, Canada.

Narayanan, S. & Yim, S.C.S 2000 Nonlinear model evaluation via system identification of a moored structural system. In *Proceedings of the 10th international offshore and polar engineering conference*. Cupertino, California, USA: III, 402-409.

Panneer Selvam, R., Bhattacharyya, S.K., & Sundaravadivelu, R. 1999 Application of R-MISO method to identify drag and inertia coefficients of a compliant SDOF system. In *Proceedings of 18th international conference of offshore mechanics and arctic engineering*, (Paper No. OMAE99 – 4071), St. John's, Canada.

Paneer Selvam, R & Bhattacharyya, S.K. 2001 Parameter identification of a nonlinear SDOF system in random ocean waves by reverse MISO method. *Ocean engineering*, **28**, 1199-1223.

Rice, H.J. & Fitzpatrick, J.A. 1991 A procedure for identification of linear and nonlinear multi-degree-of freedom system. *Journal of sound and vibration*, **149** (3), 397-411.

Spanos, P.D. & Lu, R. 1995 Nonlinear system identification in offshore structural reliablility. *Journal of OMAE*, **117**, 171-177.

Yim, S.C.S & Bartel, W.A. 1994 Nonlinear stochastic analysis phase III, part II: an investigation of the reverse MISO for identification of system parameters in a nonlinear moored sphere experiment. Port Hueneme, CA: Ocean Structures Division, Naval Facilities Engineering Service Center.

APPENDIX: R-MISO METHOD FOR NONLINEAR SDOF SYSTEM

Let the Fourier transform (FT) of the nonlinear equation of motion be

$$\sum_{i=1}^{N} A_i(\omega) X_i(\omega) = F(\omega) \qquad \text{(A1)}$$

where $X_i(\omega)$ is the FT of the input $x_i(t)$, $F(\omega)$ is the FT of the output $f(t)$ and $A_i(\omega)$ is the frequency response function of the input $x_i(t)$. This equation serves as a model for equations (4), (15), (22) and (27) for the various cases considered in this paper. Equation (A1) indicates that N inputs pass through N linear systems to produce a single output in a Multiple Input-Single Output (MISO) system. The adjective 'reversed' is due to the fact that in the actual physical problem, the excitation (input) causing response (output) is interpreted in the reverse way in equationn (A1). Thus, the nonlinear system model with a single input in the time domain is transformed into a linear model in frequency domain with multiple inputs. An equivalent form of equation (A1) can be obtained using spectral density functions. One can construct the spectral densities of the inputs and output viz., $S_{ij}(i,j = 1 \text{ to } N)$, $S_{if}(i = 1 \text{ to } N)$, and S_{ff} where subscript f stands for the 'output' f(t) and indices i and j stand for the 'inputs' $x_i(t)$ and $x_j(t)$ respectively which are related (as shown by Bendat & Piersol [1993])

$$S_{if} = \sum_{j=1}^{N} S_{ij} A_j \ , \quad i = 1,2,\ldots N. \qquad \text{(A2)}$$

where the $N \times N$ matrix is 'Hermitian' (i.e. $S_{ij} = S_{ji}^*$, where a '$*$' denotes complex conjugate). The total number of distinct spectral densities is $(N^2 - N)/2 + 2N + 1$. Equation (A2) represents a system of linear equations in unknowns $A_j (j = 1 \text{ to } N)$ which can be solved to obtain A_j, yielding the system parameters.

In general, most of the inputs and output are partially correlated. In order to obtain physically more meaningful results a 'conditioning' process has been recommended in solving MISO problems. This process results in mutually uncorrelated inputs and output. A 'coherence' plot may be constructed from the 'conditioned' data wherein the contributions of the uncorrelated inputs to the spectral output are quantified as a function of frequency. This serves as a measure of the goodness of fit of the overall model and provides a quantitative assessment of the participation of each input in the system model at various frequencies to the output (Bendat & Piersol [1993]; Rice and Fitzpatrick [1991]).

Therefore, the task now is to compute the 'conditioned' spectral densities (S_{ij}^c and S_{if}^c) which remove the correlation effects between the signals corresponding to index f (output) and indices i and j (inputs). This is accomplished [Bendat & Piersol 1993] by

$$\begin{aligned} S_{ij}^c &= S_{ij.(i-1)!} \qquad (i, j = 1 \text{ to } N) \\ S_{if}^c &= S_{if.(i-1)!} \qquad (i = 1 \text{ to } N) \end{aligned} \qquad \text{(A3)}$$

where

$$\begin{aligned} S_{ij.r!} &= S_{ij.(r-1)!} - \left[\frac{S_{rj.(r-1)!}}{S_{rr.(r-1)!}}\right] S_{ir.(r-1)!} \qquad (r < i) \\ S_{if.r!} &= S_{if.(r-1)!} - \left[\frac{S_{rf.(r-1)!}}{S_{rr.(r-1)!}}\right] S_{ir.(r-1)!} \qquad (r < i) \end{aligned} \qquad \text{(A4)}$$

In the above, $ij.r!$ and $if.r!$ mean that the spectral density between the signals with the respective indices have been 'conditioned' with respect to the signals with indices from 1 to r. In other words, the correlation effects of the signals with

indices 1 to r have been removed from S_{ij} and S_{if}. It should be noted that if $r = 0$, then $S_{ij.r!} = S_{ij}$ and $S_{if.r!} = S_{if}$.

Now, A_i^c (transfer functions based upon 'conditioned' spectral densities) can be calculated as

$$A_i^c = \frac{S_{if}^c}{S_{ii}^c}; \qquad (i = 1 \text{ to } N) \tag{A5}$$

Finally, A_i are related to A_i^c as

$$A_N = A_N^c; \quad A_i = A_i^c - \sum_{j=i+1}^{N} A_j \frac{S_{ij}^c}{S_{ii}^c}; \quad (i < N) \tag{A6}$$

The coherence functions are calculated from

$$\gamma_{if}^2 = \frac{\left|S_{if}^c\right|^2}{S_{ii}^c . S_{ff}} \tag{A7}$$

and if there is no 'noise' present in the system, then

$$\sum_{i=1}^{N} \gamma_{if}^2 = 1 \tag{A8}$$

In practical application of the technique, where the output is experimentally measured, noise will always be present in the measured output signal. Denoting this noise by $n(t)$, and the noise spectrum by S_{nn}, the coherence function relation equation (A8) stands modified as [Bendat & Piersol 1993].

$$\sum_{i=1}^{N} \gamma_{if}^2 + \frac{S_{nn}}{S_{ff}} = 1 \tag{A9}$$

The noise does not correlate with any of the inputs or the output, $S_{jn} = S_{nf} = 0$. In other words, when noise is present, the deviation from equation (A8) will indicate the noise level (S_{nn}) by virtue of equation (A9). It is to be noted that, in formulating the inputs and output of a system, none of the inputs should be 'fully correlated' to the other inputs and output for the R-MISO model to be well defined.

As an illustration, for a 'Three Input-Single Output' model ($N = 3$), equations (A3) and (A4) yield

$$S_{11}^c = S_{11}; S_{12}^c = S_{12}; S_{13}^c = S_{13}; S_{1f}^c = S_{1f} \tag{A10}$$

$$S_{22}^c = S_{22.1!} = S_{22} - \frac{S_{12}}{S_{11}} S_{21} = S_{22} - \frac{\left|S_{12}\right|^2}{S_{11}} \tag{A11}$$

(since $S_{12} = S_{21}^*$)

$$S_{23}^c = S_{23.1!} = S_{23} - \frac{S_{13}}{S_{11}} S_{21} \tag{A12}$$

$$S_{33}^c = S_{33.2!} = S_{33.1!} - \frac{S_{23.1!}}{S_{22.1!}} S_{32.1!} = S_{33} - \frac{S_{13}}{S_{11}} S_{31} - \frac{\left|S_{23}^c\right|^2}{S_{22}^c} \tag{A13}$$

$$= S_{33} - \frac{\left|S_{13}\right|^2}{S_{11}} - \frac{\left|S_{23}^c\right|^2}{S_{22}^c}$$

$$S_{2f}^c = S_{2f.1!} = S_{2f} - \frac{S_{1f}}{S_{11}} S_{21} \tag{A14}$$

and

$$S_{3f}^c = S_{3f.2!} = S_{3f.1!} - \frac{S_{2f.1!}}{S_{22.1!}} S_{32.1!} \tag{A15}$$

The 'conditioned' transfer functions follow from equation (A5) as

$$A_1^c = \frac{S_{1f}^c}{S_{11}^c}; A_2^c = \frac{S_{2f}^c}{S_{22}^c}; A_3^c = \frac{S_{3f}^c}{S_{33}^c} \tag{A16}$$

and finally, from equation (A6) we get

$$A_3 = A_3^c; A_2 = A_2^c - A_3 \frac{S_{23}^c}{S_{22}^c}; A_1 = A_1^c - A_2 \frac{S_{12}}{S_{11}} - A_3 \frac{S_{13}}{S_{11}} \tag{A17}$$

The coherence functions follow from equation (A7) as

$$\gamma_{1f}^2 = \frac{\left|S_{1f}^c\right|^2}{S_{11}^c . S_{ff}}; \tag{A18}$$

$$\gamma_{2f}^2 = \frac{\left|S_{2f}^c\right|^2}{S_{22}^c . S_{ff}}; \tag{A19}$$

$$\gamma_{3f}^2 = \frac{\left|S_{3f}^c\right|^2}{S_{33}^c . S_{ff}} \tag{A20}$$

and these obey equation (A8)

$$\gamma_{1f}^2 + \gamma_{2f}^2 + \gamma_{3f}^2 = 1 \tag{A21}$$